Journal of Innovative Technology, Vol. 4, No. 1, pp. 23-28, March 2022
http://doi.org/10.29424/JIT.202203_4(1).0004

Temporal Trends and Spatial Distribution Characteristics of Air Quality Monitored in China from 2015 to 2020

Chien-Hung Chen [1], Chang-You Tsai [1], Tu-Fu Chen [2], Li-Sian Hou [3], Ken-Hui Chang [4 *]

ABSTRACT

Pollution caused by household and industrial development affects local, national, and international air quality through meteorological conditions and atmospheric transport. Being located in the East Asian continent, and given the local weather patterns, some Chinese pollution may be transmitted to other East Asian nations. For this reason, it is necessary to perform an analysis of changes in air quality in China, to understand how other nations local to China may be affected. This study collected data from Chinese pollution monitoring stations (1641 stations in 2020), that has been released by the China National Environmental Monitoring Station network. The data was cleaned and analyzed so that trends in $PM_{2.5}$, SO_2, NO_2, and daily maximum 8-hr average ozone ($DM8O_3$) could be identified. The period examined was 2015 – 2020 and the temporal evolution and spatial variation of pollutants were analyzed. The distribution characteristics of pollutants in various regions were plotted on maps and seasonal data was also examined. During the six-year period, China's $PM_{2.5}$ and SO_2 levels showed improvement year over year; whereas the NO_2 level deteriorated at first, and then improved. Similarly, $DM8O_3$ deteriorated at first, and then improved; however, in this latter case, the overall situation was still worse at the end of the period.

Keywords: Air Quality, Temporal Variation Trend, Spatial Distribution Characteristics, Quantitative Statistic

1. INTRODUCTION

The rapid development of China's economy and the massive discharge of air pollutants over the last 30 years has led to serious air pollution incidents. This is common in many areas, and even where there is no polluting source, transport effects mean that overall air quality has deteriorated. China has formulated and introduced control policies for $PM_{2.5}$ and O_3 pollution, hoping to decrease their prevalence and improve air quality, but only with intermittent success. Pollution caused by industrial and vehicle emissions affect not only the local communities, but also overseas nations and non-local areas due to atmospheric transmission. In particular, because China is located in the East Asian continent, under certain weather patterns, its pollutants have been seen to impact other East Asian countries and regions including South Korea, Japan, Taiwan, Hong Kong, and Vietnam. China has become the primary source of overseas pollution for these countries and regions (e.g., Chen et al., 2014; Chuang et al., 2008; Koo et al., 2008; Aikawa et al., 2010; Fang et al., 1999; Shimadera et al., 2009). Analyzing the evolution of China's air quality has developed over recent years will provide an understanding of how these countries and regions are be affected.

Several related studies have already been conducted; for example, Fan et al. (2020) collected air quality monitoring data in China from 2014 to 2018. Using a spatial and time series analysis of various air pollutants they were able to show locations and AQI value ranges as they changed using a monthly time series graph. The four concentration ranges were presented in a box chart, and the study concluded with the finding that $PM_{2.5}$ concentrations were highest in winter. Silver et al. (2018) collected data from monitoring stations in China, Taiwan, and Hong Kong from 2015 to 20 17. They analyzed specific groups of particles, looking for improvement or deterioration in four main categories, $DM8O_3$, $PM_{2.5}$, NO_2, and SO_2. Over a three-year period, the spatial distribution of $PM_{2.5}$ concentrations showed little variation, but exhibited an overall improvement (in blue), some deterioration (in red), and the size of the circle was used to represent the magnitude of improvement or deterioration. The study found that from 2015 – 2017, 90% of the station concentrations showed some improvement, and 10% showed deterioration. Chu et al. (2020) studied the changes in $PM_{2.5}$ and NO_2 concentrations throughout China during the COVID-19 epidemic. To perform a pre/post comparison the data range was a specific time period (1/21 – 3/23) in the years 2015 – 2020. The study found that in 2020, the pollutant concentration levels were much lower than in previous years due to factors such as city closures.

In order to understand the recent temporal air quality trends in China, and further explore the evolutional characteristics of the spatial distribution, this study collected and analyzed air pollutant ground station monitoring data on $PM_{2.5}$, SO_2, NO_2, and daily

Manuscript received March 4, 2022; revised March 24, 2022; accepted March 31, 2022.

[1] Ph.D. student, Department of Safety, Health and Environmental Engineering, National Yunlin University of Science and Technology, Taiwan R.O.C.

[2] Assistant Researcher, Department of Safety, Health and Environmental Engineering, National Yunlin University of Science and Technology, Taiwan R.O.C.

[3] Undergraduate, Department of Safety, Health and Environmental Engineering, National Yunlin University of Science and Technology, Taiwan R.O.C.

[4*] Professor, Department of Safety, Health and Environmental Engineering, National Yunlin University of Science and Technology, Taiwan R.O.C.

maximum 8-hr average ozone ($DM8O_3$) levels. In 2020, there were 1,641 monitoring stations taking readings. From this dataset, using the hourly rates, it was possible to calculate a daily, monthly, quarterly, and annual average. Using the averages, the annual concentrations of various pollutants in China and six major regions were calculated. A quantitative analysis and a trend analysis were then performed to determine the extent of any improvement or deterioration over the past six years. Data interpolation was also used to draw a spatial distribution map of the average concentrations for the period 2015 to 2020. The distribution characteristics of pollutants for several regions in China were determined to improve the understanding of air pollution distributions across China.

2. METHOD

This research collected ground station monitoring data for various pollutants in mainland China between 2015 and 2020 for processing and analysis. The research process may be divided into three main parts: statistical observations and data collection, data pre-processing (data cleaning), and data analysis. (1) The data collection phase involved obtaining the ground station monitoring data from China's air monitoring stations for the period 2015 – 2020. This had to be broken down by types of air pollutant and geographic region. (2) Data pre-processing involved sorting and screening the downloaded data, then calculating the daily, monthly, quarterly, and annual average concentrations of $PM_{2.5}$, $DM8O_3$, NO_2, and SO_2. (3) The data output phase involved quantification and analysis of the spatial distribution characteristics and temporal trends within the data.

The monitoring station data used in this study were provided by the National Urban Air Quality Real-time Release Platform issued by the China Environmental Monitoring Station network. The original data files, along with latitude and longitude coordinates, were collated. The data types available within the files were as follows: hourly concentration values of AQI, $PM_{2.5}$, $PM_{2.5}$_24h, PM_{10}, PM_{10}_24h, SO_2, SO_2_24h, O_3, O_3_24h, O_3-8h, O_3-8h_24h, CO, CO_24h. Files were in a CSV format and required management in Compaq Visual Fortran before they could be used. The daily hourly were extracted first, then code was written to calculate the average concentration for each time period. The definitions and calculation method were as follows:

(1) Daily average concentration value: for each station, calculate the arithmetic mean of the 24-hour average concentrations for the day. Where a day contains less than 16 hours, the data is regarded as invalid.

(2) Monthly average concentration value: calculate the arithmetic mean of the effective daily average concentration of each given pollutant at the same station in that month. The obtained value is treated as the monthly average concentration value. Where a month contains less than 20 days, the data is regarded as invalid.

(3) Seasonal average concentration value: calculate the arithmetic average of the effective daily average concentration of each given pollutant at the same station in that season. The obtained value is treated as the quarterly average concentration value. Where a quarterly value contains less than 60 days, the data is regarded as invalid. In this study, March to May was regarded as spring; June to August was summer; September to November was autumn; December and January to February of the same year was winter.

(4) Annual average concentration value: calculate the arithmetic average of the effective daily average concentration of each given pollutant at the same station in that year. Where a year contains less than 250 days, the data is considered invalid.

In the period 2015 – 2017, the number of air quality stations in China (excluding traffic stations) was 1,497. In 2018 this number increased 1,605. By 2020 this number had increased again to 1,641. Figure 1 shows the spatial distribution of all 1,641 atmospheric monitoring stations in mainland China in 2020.

In this study, the seasonal and annual average concentrations of air pollutants calculated by the above methods at the stations indicated in Figure 1 were interpolated by the Kriging method. The average annual spatial distribution map was constructed to determine the spatial distribution characteristics of each pollutant concentration and variety. Then, the monthly average concentration values of each air pollutant were drawn into a monthly average time-series graph that was able to depict the proportion of each pollutant. This makes it possible to quantitatively analyze the seasonal fluctuations in each pollutant, and observe changes in pollutant proportions over time.

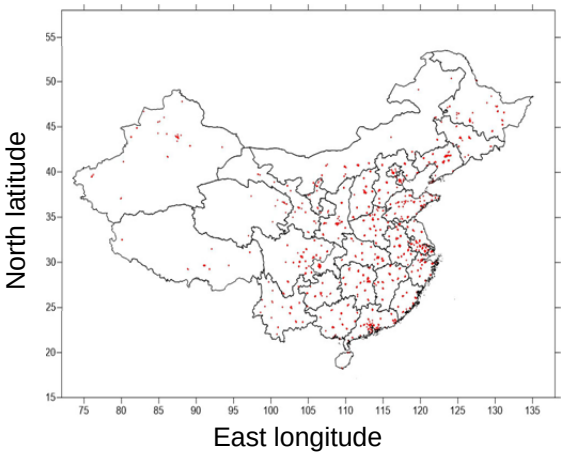

Fig. 1 Spatial distribution of 1641 air quality monitoring sites over the whole China in 2020

3. RESULTS AND DISCUSSION

3.1 $PM_{2.5}$

The spatial distribution map of the annual average $PM_{2.5}$ concentration from 2015 to 2020 is shown in Figure 2. From the perspective of spatial distribution, the places with higher $PM_{2.5}$ concentrations in China in 2015 were concentrated in the Beijing-Tianjin-Hebei region in North China, and the western region Xinjiang. The concentration in the Beijing-Tianjin-Hebei region decreased compared with previous years. In 2019, it was observed that pollution conditions in both the Xinjiang and Tibetan Autonomous Regions had deteriorated. By 2020, the Beijing-Tianjin-Hebei region showed higher concentrations, but the Xinjiang region had shown improvement.

Table 1 shows the annual average $PM_{2.5}$ concentration data and the statistics from the China Air Quality Monitoring Stations between 2015 and 2020. The annual average concentration of $PM_{2.5}$ in China improved year over year, from 52.1 μg/m³ in 2015 to 34.4 μg/m³ in 2020. In the six major regions, only the northwest in 2016 and the northeast in 2019 saw any increase in $PM_{2.5}$ concentrations. Overall, the $PM_{2.5}$ concentrations in China

declined over the six year period. The major region showing most improvement was southern China.

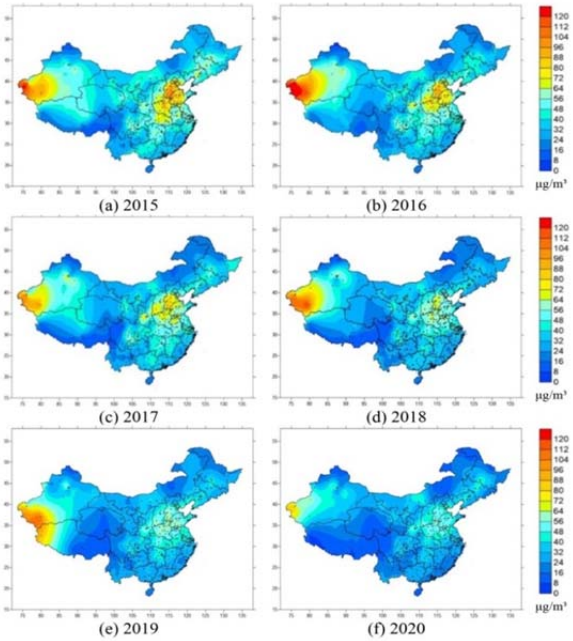

Fig. 2 Spatial distributions of the annual average of $PM_{2.5}$ concentration in China for the past 6 years from 2015 to 2020.

Table 1 Annual average of $PM_{2.5}$ concentration in various regions of China from 2015 to 2020

	Annual average of $PM_{2.5}$ concentration (μg/m³)						Difference of 2020 and 2015	
	2015 (A)	2016 (B)	2017 (C)	2018 (D)	2019 (E)	2020 (F)	Conc. (μg/m³) (F-A)	Ratio (%) (F-A) /A
East China	53.8	48.6	46.6	41.7	39.6	34.4	-19.4	-36.1
South China	53.0	47.6	46.0	41.8	38.8	33.6	-19.4	-36.6
North China	61.1	58.7	56.4	49.4	44.6	41.1	-20.0	-32.7
Southwest China	40.6	39.8	35.4	32.5	30.3	27.9	-12.7	-31.3
Northeast China	51.7	42.2	41.6	34.2	35.5	34.7	-17.0	-32.9
Northwest China	50.2	52.9	49.8	45.3	40.8	37.3	-12.9	-25.7
Whole China	52.1	48.1	45.9	40.9	38.4	34.4	-17.7	-33.9

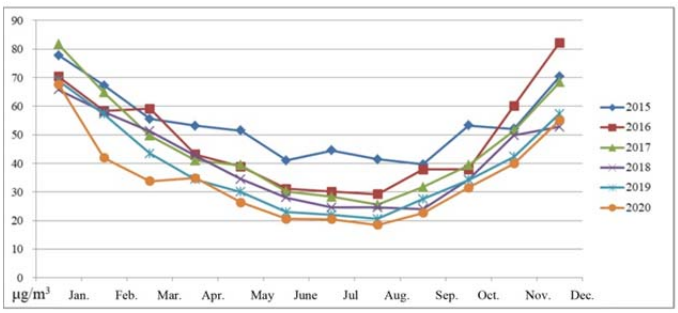

Fig. 3 Monthly variation of averaged $PM_{2.5}$ concentration over China for the past 6 years from 2015 to 2020.

Fig. 3 shows a time series representation of the monthly $PM_{2.5}$ data. From this chart, it can be seen that concentrations were consistently and reliably higher in winter and lower in summer. The monthly average concentration also decreased each year. A notable observation in Fig. 3 is the 2020 year (orange), where the January to March data shows an unusually low reading. This can be accounted for by the decreased industrial activity during the COVID-19 outbreak, where the concentrations dropped from 70 μg/m³ in January, to 32 μg/m³ by March.

The $PM_{2.5}$ pollution levels shown in Fig. 4 showed an increasing number of green ($\leqq 35\ \mu g/m^3$) days. This occurred across China, and the six major regions had followed this trend. In North China in 2015, pollution levels were usually higher, often falling into the red category (> 115 μg/m³). The proportion of pollution days with red levels was about 10%, but by 2020 this was less than 5 %. This is a significant improvement in $PM_{2.5}$ concentrations over the period studied.

3.2 Daily Maximum 8-hr Average O_3 ($DM8O_3$)

The spatial distribution of the annual average concentration of Daily Maximum 8-hr Average Ozone ($DM8O_3$) from 2015 to 2020 is shown in Figure 5. The areas with higher $DM8O_3$ concentrations in 2015 and 2016 were in Gansu, Qinghai Province, Beijing-Tianjin-Hebei, and the Yangtze River Delta. In 2017 and 2018, the North China region deteriorated significantly overall, with average annual concentrations of more than 100 μg/m³. By 2020, the high-concentration areas had decreased, and the overall concentration in Beijing, Tianjin and Hebei had also improved; however, there were still areas where the concentration exceeded 100 μg/m³. Air quality in Tibet had also deteriorated. Examining Figures 5(a) through Figure 5(f), it can be seen that in 2020 there $DM8O_3$ levels had been increasing generally. The most notable areas of increase were in North China and some Eastern provinces, in addition to Xinjiang and Tibet. However, 2020 again shows improvement when compared to 2019 (Figure 5(e)). Almost all of the $DM8O_3$ readings exhibited some improvement, the only places that deteriorated were some northwestern regions. Areas showing the most obvious improvement were Yunnan and Hunan province.

The annual average $DM8O_3$ concentration data for the period 2015 to 2020 is presented in Table 2. The annual average concentration of $DM8O_3$ in China was deteriorated from 83.2 μg/m³ in 2015 to 95.7 μg/m³ in 2018 and then improved from 93.3 μg/m³ in 2019 to 90.6 μg/m³ in 2020. The annual average values in the six major regions were almost highest in 2018, and then decreased except for the Northeast, where air quality deteriorated in 2020. Over the six-year period, $DM8O_3$ levels got worse across China by 8.9%, but the most heavily affected area was North China where the level increased by 16.3%. The last two years of data showed that generally the situation had improved, and only the Northeast region had deteriorated, where the deterioration rate was 1.3%. In South China the $DM8O_3$ levels improved by 6.2%. Between 2015 and 2018, the greatest increase in $DM8O_3$ levels was 23.8% in North China. The greatest improvement in the period 2018-2020 was 6.4% in Southwest China.

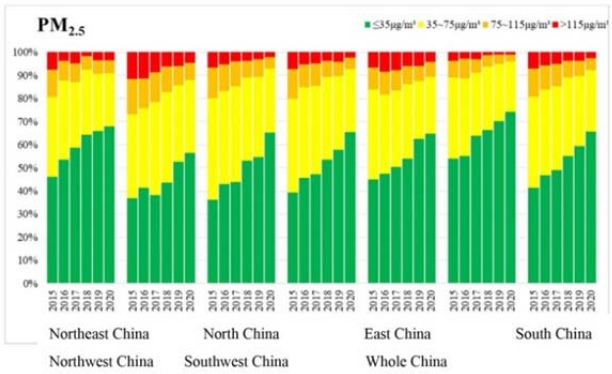

Fig. 4 The ratios of various $PM_{2.5}$ pollution levels for various regions in China from 2015 to 2020

Table 2 Annual average of $DM8O_3$ concentration in various regions of China from 2015 to 2020

	Annual average of $DM8O_3$ concentration (μg/m³)						Difference of 2020 and 2015	
	2015 (A)	2016 (B)	2017 (C)	2018 (D)	2019 (E)	2020 (F)	Conc. (μg/m³) (F-A)	Ratio (%) (F-A) /A
East China	86.7	90.9	101.0	101.4	99.8	96.7	10.0	11.5
South China	83.2	86.0	91.1	94.1	94.0	88.2	5.0	6.0
North China	84.6	90.1	104.2	104.7	101.5	98.4	13.8	16.3
Southwest China	77.0	79.6	82.7	85.8	81.1	80.3	3.3	4.3
Northeast China	81.6	83.5	89.4	87.4	83.0	84.1	2.5	3.1
Northwest China	81.9	88.5	95.2	95.5	91.6	91.0	9.1	11.1
Whole China	83.2	86.9	94.5	95.7	93.3	90.6	7.4	8.9

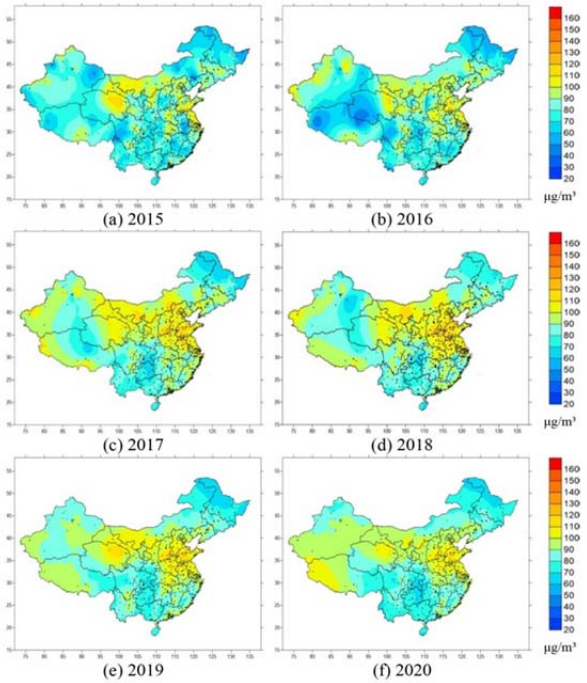

Fig. 5 Spatial distributions of the annual average of $DM8O_3$ concentration in China for the past 6 years from 2015 to 2020

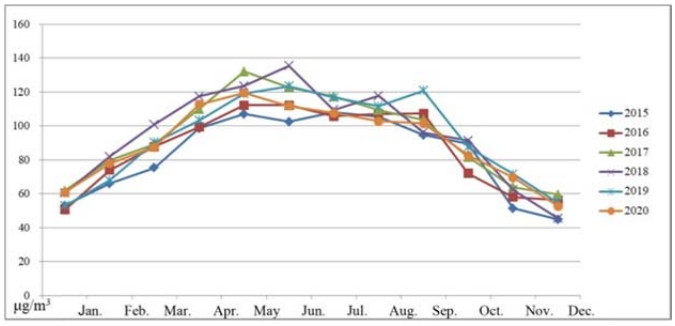

Fig. 6 Monthly variation of averaged $DM8O_3$ concentration over China for the past 6 years from 2015 to 2020

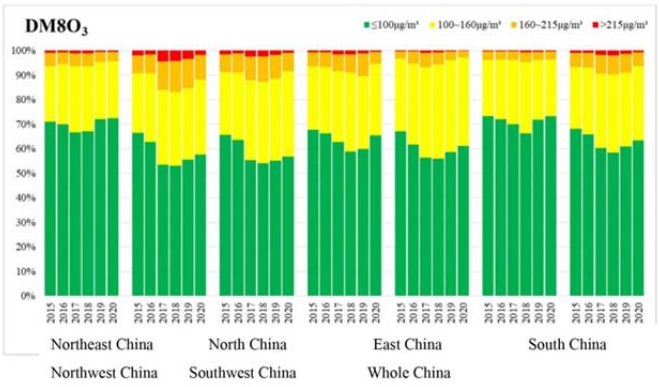

Fig. 7 The ratios of various $DM8O_3$ pollution levels for various regions in China from 2015 to 2020

Table 3 Annual average of NO_2 concentration in various regions of China from 2015 to 2020

	Annual average of NO_2 concentration (μg/m³)						Difference of 2020 and 2015	
	2015 (A)	2016 (B)	2017 (C)	2018 (D)	2019 (E)	2020 (F)	Conc. (μg/m³) (F-A)	Ratio (%) (F-A) /A
East China	33.6	33.6	34.6	32.0	31.2	27.9	-5.7	-17.0
South China	30.0	30.0	30.6	28.9	27.0	23.3	-6.7	-22.3
North China	37.6	39.5	40.6	36.8	35.3	32.0	-5.6	-14.9
Southwest China	25.8	26.6	27.1	25.5	24.4	22.2	-3.6	-14.0
Northeast China	31.8	29.2	29.1	26.1	24.9	24.0	-7.8	-24.5
Northwest China	31.2	33.0	34.9	31.7	30.6	27.6	-3.6	-11.5
Whole China	31.7	31.9	32.7	30.3	28.9	26.2	-5.5	-17.5

Table 4 Annual average of SO_2 concentration in various regions of China from 2015 to 2020

	Annual average of SO_2 concentration (μg/m³)						Difference of 2020 and 2015	
	2015 (A)	2016 (B)	2017 (C)	2018 (D)	2019 (E)	2020 (F)	Conc. (μg/m³) (F-A)	Ratio (%) (F-A) /A
East China	25.5	21.3	17.0	12.6	10.2	9.0	-16.5	-64.7
South China	21.3	17.9	14.2	11.6	9.2	8.4	-12.9	-60.6
North China	41.4	38.7	32.3	21.4	16.6	13.5	-27.9	-67.4
Southwest China	17.2	15.3	13.2	11.1	9.2	8.5	-8.7	-50.6
Northeast China	32.2	27.0	22.1	16.9	15.4	13.5	-18.7	-58.1
Northwest China	24.4	21.2	19.0	15.1	11.4	10.6	-13.8	-56.6
Whole China	25.9	22.3	18.4	14.0	11.2	10.0	-15.9	-61.5

Fig. 6 is a time series chart showing changes in $DM8O_3$ levels. There are some obvious seasonal differences between this data and the earlier $PM_{2.5}$ data in Fig. 5. Here, concentrations are higher in summer, and the highest monthly average concentration is found between May and September. The main reason for this is the intensity of sunlight in summer increasing the photochemical reaction which leads to ozone. In 2018, there were large fluctuations throughout the year. 2018 also happened to be the year with the highest average annual concentration. The monthly averages were stable in 2020, but the concentrations were still higher than in 2015.

Fig. 7 shows that the number of excellent ($\leqq 160\ \mu g/m^3$) days with low $DM8O_3$ pollution levels in the six major regions decreased annually between 2015 and 2018, but increased in 2019 and again in 2020. The increases in North China during 2017 and 2018 caused greatest rise in number of days, as the number of moderate (>215 μg/m³) days was significantly higher than for the other years. In South China, some pollution increases found in 2019 did not decline until 2020.

3.3 NO_2

Figure 8 shows the spatial distribution of the annual average NO_2 concentrations in China from 2015 – 2020. Areas with higher average NO_2 concentrations from 2015 to 2017 were mainly in Shandong Province, and other highly developed areas such as Beijing-Tianjin-Hebei and the Yangtze River Delta. Concentrations were approximately 55 μg/m³ in 2017 in Anhui Province, and this increased over time. Concentrations in Beijing-Tianjin-Hebei declined slightly in 2018 and 2019. By 2020, the overall average annual concentrations in Beijing-Tianjin-Hebei had fallen below 40 μg/m³. Overall, the annual average concentration of NO_2 showed improvement significantly over the period 2015 – 2020, especially in Xinjiang, Beijing-Tianjin-Hebei, and the Yangtze River Delta.

Table 3 presents the data for NO_2 pollution levels from 2015 – 2020. The annual average concentration of NO_2 in China was getting worse from 31.7 μg/m³ in 2015 to 32.7 μg/m³ in 2017 and then improved from 30.3 μg/m³ in 2018 to 26.2 μg/m³ in 2020. In that period overall, NO_2 levels increased. 2017 showed the highest average values, but after 2017 NO_2 levels improved. 2020 had the lowest values of the six-year period. Across China, NO_2 levels in the six major regions first increased, then decreased. The exception to this was Northeast China, which improved every year. Over the period 2015 – 2020, all six regions showed improvement. The overall decrease in NO_2 was 17.5%, and the Northeast region showed the greatest decrease of 24.5%. The 2019 – 2020 data showed improvements in all six major regions, but the greatest decrease was 13.7% in South China.

3.4 SO_2

Figure 9 shows a spatial distribution of the annual average SO_2 concentrations in China from 2015 to 2020. In that period, SO_2 levels across China decreased, especially in areas surrounding Beijing-Tianjin-Hebei and other high-pollution areas such as Xinjiang. The areas with higher concentrations in 2015 and 2016 were North China and Xinjiang, where the annual average value was more than 39 μg/m³. In 2017, the areas with high concentrations decreased, leaving only Shanxi Province and its surrounding areas with similar, but lower values. The concentrations in Xinjiang and Shanxi continued to decline in 2018 and 2019. By 2020, the overall concentration in Shanxi had dropped to below 24 μg/m³. The annual average concentration of SO_2 in other regions of China was below 18 μg/m³. The overall improvement was notable.

Table 4 presents the annual average SO_2 concentration data for the period 2015 – 2020. The annual average SO_2 concentration in China and the six major regions had improved annually and there was no increase. The annual average concentration of SO_2 in China decreased from 25.9 μg/m³ in 2015 to 10.0 μg/m³ in 2020. The overall improvement was visible in the data as it dropped by 61.5%. The area with the greatest improvement was North China, in which the SO_2 concentration declined by 67.4%.

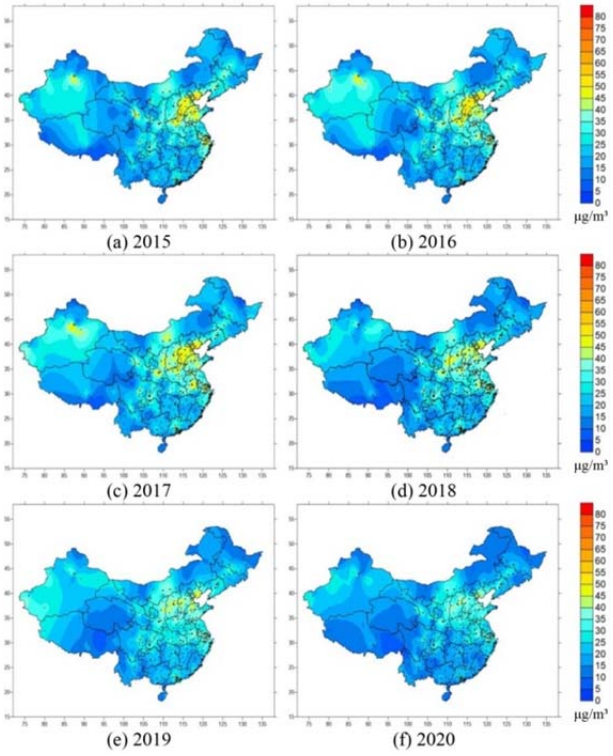

Fig. 8 Spatial distributions of the annual average of NO_2 concentration in China for the past 6 years from 2015 to 2020

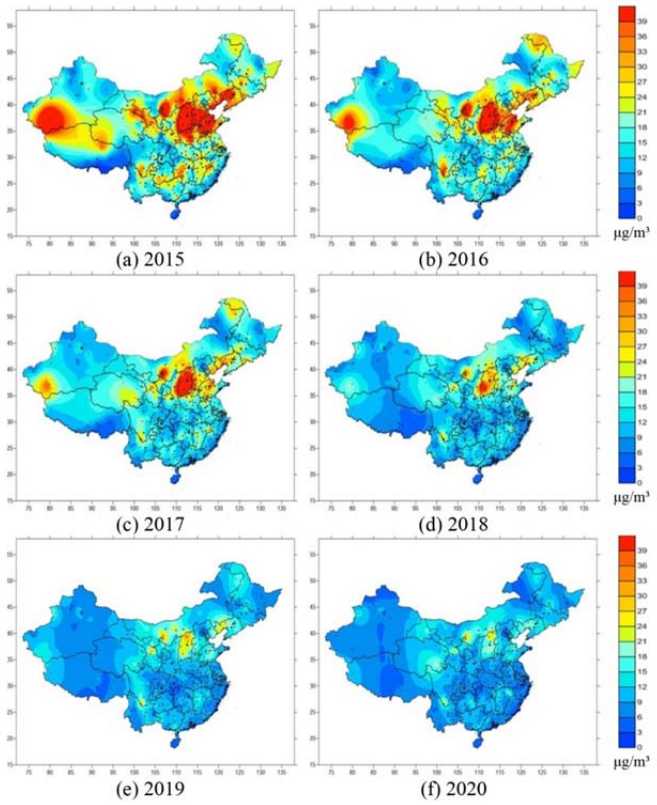

Fig. 9 Spatial distributions of the annual average of SO_2 concentration in China for the past 6 years from 2015 to 2020

4. CONCLUSION

This paper examined pollution data from across China for the period 2015 – 2020. During the period, $PM_{2.5}$ and $DM8O_3$ were the main pollutants. Other sources of pollution remained at relatively low levels. $PM_{2.5}$ was mainly concentrated in North China and Xinjiang province. Beijing-Tianjin-Hebei region was the largest economic area in the dataset and is located in the North China Plain. During the winter months, it is common for people in that region to burn fossil fuels for heat, leading to increased pollution levels. Compounding this issue, rainfall is less common and convective activity is weaker, both of these make it harder for the air to diffuse high pollution levels. In recent years, many regions have implemented pollution mitigation or prevention strategies such as "coal-to-gas" and "coal-to-electricity", in order to reduce air pollution during the winter period. This is also to fall in-line with national emission reduction policies. These policies have apparently had some effect on pollution levels as there is a decreasing trend year over year. The annual average concentration of $PM_{2.5}$ in China improved year over year, from 52.1 μg/m³ in 2015 to 34.4 μg/m³ in 2020. The area showing most improvement was southern China. The similar trend are also shown for the annual average concentration of SO_2 in China improved from 25.9 μg/m³ in 2015 to 10.0 μg/m³ in 2020, associated with the most improvement area North China. However, the different trends were presented for $DM8O_3$ and NO_2. The annual average concentration of NO_2 in China was getting worse from 31.7 μg/m³ in 2015 to 32.7 μg/m³ in 2017 and then improved from 30.3 μg/m³ in 2018 to 26.2 μg/m³ in 2020; while that of $DM8O_3$ in China was deteriorated from 83.2 μg/m³ in 2015 to 95.7 μg/m³ in 2018 and then improved from 93.3 μg/m³ in 2019 to 90.6 μg/m³ in 2020.

The most significant pollution source $DM8O_3$, was mainly concentrated in North China. This is attributable to the dense population and the rapid development in this area. The population growth and intensive industrial emissions combine with local meteorological conditions to create deteriorating air quality. The improvement of ozone levels requires a coordinated approach to reduce the emission of ozone's precursors including NO_2. Where emission controls are paired with an understanding of pollutant precursors, the combination of information and policy will hopefully lead to lasting improvements in air quality.

REFERENCE

Aikawa, M., Ohara, T., Hiraki, T., Oishi, O., Tsuji, A., Yamagami, M., Murano, K., Mukai, H., (2010). "Significant geographic gradients in particulate sulfate over Japan determined from multiple-site measurements and a chemical transport model: Impacts of transboundary pollution from the Asian continent." *Atmospheric Environment* **44**, 381-391.

Chen, T.-F., Chang, K.-H., Tsai, C.-Y., (2014). "Modeling direct and indirect effects of long range transport on atmospheric $PM_{2.5}$ levels," *Atmospheric Environment*, **89**, 1-9.

Chu, B., Zhang, S., Liu, J., Ma, Q., He, H., (2021). "Significant concurrent decrease in $PM_{2.5}$ and NO_2 concentrations in China during COVID-19 epidemic." *Journal of environmental Science* **99**, 346-353.

Chuang, M.T., Fu, J.S., Jang, C.J., Chan, C.C., Ni, P.C., Lee, C.T., (2008). "Simulation of longrange transport aerosols from the Asian Continent to Taiwan by a Southward Asian high-pressure system." *Science of Total Environment* **406**, 168-179.

Fan, H., Zhao, C., Yang, Y., (2020). "A comprehensive analysis of the spatio-temporal variation of urban air pollution in China during (2014–2018)." *Atmospheric Environment* 220, 117066.

Fang, M., Zheng, M., Wang, F., Chim, K.S., Kot, S.C., (1999). "The long-range transport of aerosols from northern China to Hong Kong e a multi-technique study." *Atmospheric Environment* **33**, 1803-1817.

Koo, Y.S., Kim, S.T., Yun, H.Y., Han, J.S., Lee, J.Y., Kim, K.H., Jeon, E.C., (2008). "The simulation of aerosol transport over East Asia region." *Atmospheric Research* **90**, 264-271.

Li, K., Jacob, D.J., Liao, H., Shen, L., Zhang, Q., Bates, K.H., (2019). "Anthropogenic drivers of (2013–2017) trends in summer surface ozone in China." *Proceedings of the National Academy of Sciences*, **116**(2) 422–427.

Shimadera, H., Kondo, A., Kaga, A., Shrestha, K.L., Inoue, Y., (2009). "Contribution of transboundary air pollution to ionic concentrations in fog in the Kinki Region of Japan." *Atmospheric Environment* 43, 5894-5907.

Silver, B., C L Reddington, C.L., Arnold, S.R., Spracklen, D.V., (2018). "Substantial changes in air pollution across China during (2015–2017)." *Environmental Research Letters* 13, 114012.